

# Numerical simulation traffic-related air pollution : Effect of horizontal wind shear

Anis CHAARI<sup>1,\*</sup>, Waleed MOUHALI<sup>1</sup>, Nacer SELLILA<sup>2</sup>, Mohammed LOUAKED<sup>3</sup>, and Houari MECHKOUR<sup>1</sup>

<sup>1</sup>LyRIDS, ECE-Paris Engineering School, 10 Rue Sextius Michel, 75015 Paris, France

<sup>2</sup>IFSTTAR Marne la Vallée, Université Gustave Eiffel, 5 Boulevard Descartes, 77420 Champs-sur-Marne, Cedex 2

<sup>3</sup>Laboratoire de Mathématiques Nicolas Oresme, Université de Caen, Campus II, Bd. Maréchal Juin, 14032 Caen, France

**Abstract.** The concentration of emissions related to traffic in urban areas is influenced by meteorological factors, particularly horizontal wind shear and the temporal and spatial dependence of wind velocity magnitude. We have developed a two-dimensional mathematical model to address the traffic flow/pollution coupled problem, where pollution source is generated by the density of vehicles. Its numerical solution is calculated using an algorithm that combines the Lagrange Galerkin method for spatial discretization and the Characteristic method for temporal discretization. A single direction and varying wind velocity magnitudes are examined in order to determine how the presence of an obstacle affects the distribution of pollutant concentration in a bifurcation topology traffic. We have also studied the temporal evolution of pollutant concentration at several pertinent locations within the domain for two wind velocities. Different transport pollution regimes have been observed depending on time and wind direction.

## 1 Introduction

Road traffic is a major source of air pollution and greenhouse gas emissions, particularly in densely populated cities like Paris, where highways run close to residential areas. Understanding pollutant transport dynamics in urban settings is crucial for effective air quality management [1].

Computational Fluid Dynamics (CFD) simulations have been widely used to study traffic-related pollution, analyzing its dispersion at intersections, the influence of avenue trees, and the role of meteorological factors like wind shear (see for example [2]). Wind shear significantly affects pollutant dispersion, with moderate shear enhancing vertical mixing and strong shear creating turbulence, leading to complex dispersion patterns. While much research has focused on vertical wind shear, horizontal shear remains underexplored, despite its impact on long-range pollutant transport and nocturnal ozone pollution [3].

Recent CFD advancements, combined with experimental approaches, have improved urban air quality modeling. Studies have also assessed how green infrastructure mitigates pollution under varying traffic and wind conditions, informing urban planning strategies (see [4], [5], [6]). However, they do not directly account for the significant influence of instantaneous wind dynamics and their impact on sensor-based monitoring analysis.

This study expands on existing research by examining horizontal wind shear effects on pollutant dispersion through a two-dimensional traffic flow model. Unlike conventional methods with predefined pollution sources, this approach directly links emissions to traffic dynamics, offering a more realistic representation of pollution patterns. This work introduces a traffic obstacle to simulate congestion, with the primary goal of analyzing pollutant dispersion over time and space, as well as assessing concentration levels at varying distances from

---

\*e-mail: [anis.chaari@ece.fr](mailto:anis.chaari@ece.fr)

the source. A secondary objective is to investigate the characterization and effects of eddies on pollutant transport.

The paper is organized as follows. Section 2 describes the coupled model traffic flow/pollution whose pollution source is generated by the density of vehicles. Section 3 is devoted to expose the numerical methods and approximations used to solve the coupled spatio-temporal equations. In Section 4, the results of numerical simulations are presented and analysed for a portion of road before concluding in section 5.

## 2 Mathematical formulation of the problem

### 2.1 2D traffic flow model

We consider a metropolitan region where the road network is sufficiently dense to be approximated as a continuum, allowing cars to go at any location  $(x, y)$  on the two-dimensional network.  $\Omega$  and  $\Gamma$  represent this road network and its border, respectively. Here, the inflow boundary is represented by  $\Gamma_{in}$ , the outflow boundary by  $\Gamma_{out}$ , and the boundary of inaccessible areas or barriers by  $\Gamma_0$ .  $L$  is the road network's characteristic length. Thus,  $\Gamma = \Gamma_0 \cup \Gamma_{in} \cup \Gamma_{out}$  similar to the one shown in Figure 1.

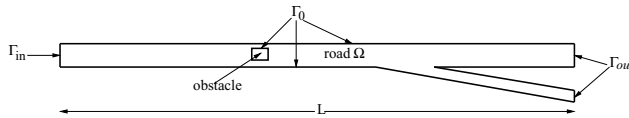


**Figure 1.** Road network  $\Omega$  (road + bifurcation).

2D continuous and dynamic models, based on a conservation law, can be used to simulate the dense traffic in urban areas. The traffic density  $\rho(x, y, t)$ , that varies with time  $t$ , is represented as a variable on a plane  $(x, y) \in \Omega$ . The dynamic advection-diffusion equation with its conditions allowing to compute this density is given by [7, 8]:

$$\left\{ \begin{array}{ll} \frac{\partial \rho}{\partial t} + \nabla \cdot \mathbf{F} = 0 & \text{in } \Omega \times (0, T), \\ \mathbf{F} = \rho \mathbf{v} - k \nabla \rho & \text{in } \Omega \times (0, T), \\ \mathbf{v} = v_{max} \left( 1 - \exp \left( \frac{c}{v_{max}} \left( 1 - \frac{\rho_{max}}{\rho} \right) \right) \right) \mathbf{d}_\theta & \text{in } \Omega \times (0, T), \\ \rho(x, y, 0) = \rho^0(x, y) & \text{in } \Omega, \\ k \frac{\partial \rho}{\partial \mathbf{n}} = f_{in} + \rho \mathbf{v} \cdot \mathbf{n} & \text{on } \Gamma_{in} \times (0, T), \\ k \frac{\partial \rho}{\partial \mathbf{n}} = 0 & \text{on } (\Gamma_{out} \cup \Gamma_0) \times (0, T), \end{array} \right. \quad (1)$$

where  $\mathbf{F}$  [in veh/km/h] is the traffic flow vector,  $k$  is a positive diffusion coefficient,  $v_{max}$  is the maximum velocity,  $c$  is a velocity that determines how rapidly the velocity magnitude decreases with increasing density,  $\rho_{max}$  is the maximum density,  $\mathbf{d}_\theta(x, y) = (\cos(\theta(x, y)), \sin(\theta(x, y)))$  is the direction vector with  $\theta$  the angle between  $\mathbf{d}_\theta$  and the x-axis,  $\rho^0$  is the initial density,  $f_{in}(x, y, t)$  is the vehicle flow rate at  $\Gamma_{in}$ ,  $\mathbf{n}$  is the outward unit normal vector to the boundary of  $\Omega$ ,  $T$  is the duration of the simulation and  $\mathbf{v}$  is the velocity of vehicle flow verifying  $\mathbf{v} \cdot \mathbf{n} = 0$  on  $\Gamma_0$ ,  $\mathbf{v} \cdot \mathbf{n} < 0$  on  $\Gamma_{in}$  and  $\mathbf{v} \cdot \mathbf{n} > 0$  on  $\Gamma_{out}$ .

The displacement of vehicles at their velocity  $\mathbf{v}$  is described by the advective flow  $\rho \mathbf{v}$ . Road traffic density affects this velocity, which is calculated a priori using the third expression of (1). Additionally,  $-k \nabla \rho$  denotes a diffusive flow that was included to mitigate the abrupt variations in velocity and density between the various regimes. It describes how cars adjust

their velocities to the traffic circumstances around them. Therefore, it can be said that the diffusion phenomenon in urban traffic is consistent with user behavior [8].

Under certain regularity conditions, the first two equations of (1) can be written in the following form :

$$\frac{\partial \rho}{\partial t} + \mathbf{v} \cdot \nabla \rho + \rho \nabla \cdot \mathbf{v} - k \Delta \rho = 0 \quad \text{in } \Omega \times (0, T). \tag{2}$$

Note that equation will be used for numerical approximation in section 3. The constant  $k$  represents the amount of flow variation as a function of the density gradient. Its value depends mainly on many traffic parameters, the weather and the driver's behavior. The value of the parameter  $c$  is significantly affected by the critical density  $\rho_c$ . The third equation of 1 represents the concave Macroscopic Fundamental Diagram proposed by Newell [9] and Francklin [10]. For  $k = 0$ , we find the two-dimensional LWR model introduced by Mollier [11].

### 2.2 Macroscopic pollution model

To visualize the distribution of the traffic-related air pollution outside of  $\Omega$ , we consider a larger region denoted by  $\Omega_p$  (including  $\Omega$ ) of boundary  $\Omega_p$ , of characteristic length  $L$  and width  $W$  (see figure 2). The model of traffic flow is coupled with a macroscopic air pollution

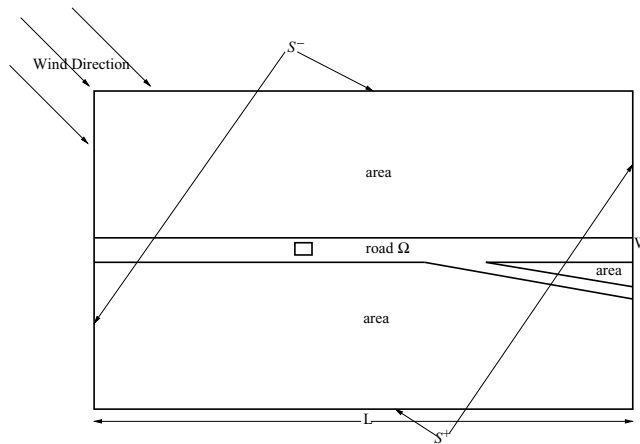


**Figure 2.** Region  $\Omega_p$  including the road network  $\Omega$

model whose pollution source is generated by density of vehicles. The density  $\rho$  and the traffic flow norm  $\|\mathbf{F}\|$  are the main factors which affect the source of pollution  $Q$  [in  $\text{kg}/\text{km}^2/\text{h}$ ] on  $\Omega$  defined as the Radon measure by:

$$Q(\cdot, t) : C(\overline{\Omega}) \longrightarrow \mathbb{R} \tag{3}$$

$$v \longmapsto \langle Q(\cdot, t), v \rangle = \int_{\Omega} (\eta \rho(x, y, t) + \nu \|\mathbf{F}\|) v(x, y) d\Omega,$$

for each  $t \in (0, T)$ , where  $C(\overline{\Omega})$  is the set of continuous functions equipped with the usual scalar product  $\langle \cdot, \cdot \rangle$ , and  $\eta$  and  $\nu$  are parameters representing contamination rates. For more details on the Radon measure, we refer the reader to the book of [12] in section 4.1.5.

To simulate traffic-related air pollution, we use a mathematical model proposed in [13]. The spatial and temporal evolution of the pollutant concentration  $\phi(x, y, t)$  can be computed

by solving the convection diffusion pollution model which is written as :

$$\begin{cases} \frac{\partial \phi}{\partial t} + \mathbf{u} \cdot \nabla \phi + \sigma \phi - \mu \Delta \phi = Q & \text{in } \Omega_p \times (0, T), \\ \phi(x, y, 0) = \phi^0(x, y) & \text{in } \Omega_p, \\ \mu \frac{\partial \phi}{\partial \mathbf{n}} = \phi \mathbf{u} \cdot \mathbf{n} & \text{on } S^-, \\ \mu \frac{\partial \phi}{\partial \mathbf{n}} = 0 & \text{on } S^+, \end{cases} \quad (4)$$

where the field  $\mathbf{u}(x, y, t)$  is the wind velocity,  $\sigma > 0$  is the extinction rate,  $\mu > 0$  is the molecular diffusion coefficient [14],  $\phi^0(x, y)$  is the initial concentration,  $S^- = \{(x, y, t) \in \Gamma_p \times (0, T) \text{ such that } \mathbf{u} \cdot \mathbf{n} < 0\}$  represents the inflow of  $\Gamma_p$  and  $S^+ = \{(x, y, t) \in \Gamma_p \times (0, T) \text{ such that } \mathbf{u} \cdot \mathbf{n} \geq 0\}$  is the outflow of  $\Gamma_p$  with  $\Gamma_p = S^- \cup S^+$  as explained in Figure 2.

### 3 Numerical approach

The coupled space-time equations (1)-(3)-(4) are solved numerically by an algorithm that combines the  $\mathbb{P}^1$  Lagrange-Galerkin method for the spatial discretization with the characteristics method for the temporal discretization [15]. The interval  $(0, T)$  is divided into  $N$  subintervals of length  $\Delta t = T/N$ . Then,  $\rho^n$  is the density of traffic and  $\phi^n$  the pollutant concentration at time  $t^n$  for  $n = 0, \dots, N$ .

We consider a triangular discretization of  $\Omega_p$  and two finite element spaces:  $U_h$  for density and  $V_h$  for concentration [16]. Let  $\rho_h^0 \in U_h$  and  $\phi_h^0 \in V_h$ , we must find  $\rho_h^{n+1} \in U_h$  and  $\phi_h^{n+1} \in V_h$ , for  $n = 0, \dots, N - 1$ , such that

$$\begin{aligned} & \int_{\Omega} \frac{\rho_h^{n+1} - \rho_h^n \circ X_h^n}{\Delta t} u_h \, d\Omega + \int_{\Omega} \rho_h^{n+1} (\nabla \cdot \mathbf{v}_h^n) u_h \, d\Omega + \int_{\Omega} k \nabla \rho_h^{n+1} \cdot \nabla u_h \, d\Omega \\ & - \int_{\Gamma_{in}} (f_{in}^{n+1} + \rho_h^{n+1} \mathbf{v}_h^n \cdot \mathbf{n}) u_h \, d\Gamma_{in} = 0, \quad \forall u_h \in U_h, \end{aligned} \quad (5)$$

and

$$\begin{aligned} & \int_{\Omega_p} \frac{\phi_h^{n+1} - \phi_h^n \circ X_h^n}{\Delta t} v_h \, d\Omega_p + \int_{\Omega_p} \sigma \phi_h^{n+1} v_h \, d\Omega_p + \int_{\Omega_p} \mu \nabla \phi_h^{n+1} \cdot \nabla v_h \, d\Omega_p \\ & - \int_{S^-} \phi_h^{n+1} \mathbf{u}^{n+1} \cdot \mathbf{n} v_h \, dS^- = \int_{\Omega_p} (\eta \rho_h^{n+1} + \nu \|\mathbf{F}\|) v_h \, d\Omega_p, \quad \forall v_h \in V_h, \end{aligned} \quad (6)$$

where  $X_h^n$  is an approximation of  $X^n(x, y) = X(x, y, t^{n+1}; t^n)$  defining the position of the particle at instant  $t^n$  that was in  $(x, y)$  at the instant  $t^{n+1}$ ,  $\mathbf{v}_h^n$  is an approximation of  $\mathbf{v}^n$  and  $u_h$  and  $v_h$  are the test functions in the finite element spaces  $U_h$  and  $V_h$ , respectively. The software FreeFem++ is used to calculate the solutions  $\rho_h^{n+1}$  and  $\phi_h^{n+1}$  [17].

### 4 Numerical results

For simulations, we choose a portion of the northern ring road of Paris ("Périphérique de Paris")  $\Omega$  of characteristic length  $L = 1$  km. The inflow boundary  $\Gamma_{in}$  measures  $14 \cdot 10^{-3}$  km.  $\Gamma_{out}$  measures  $14 \cdot 10^{-3}$  km for the exit at the top and  $7 \cdot 10^{-3}$  km for the exit at the bottom. To have a sufficiently dense traffic, we have implanted a rectangular obstacle in the middle of the network at 0.4 km of  $\Gamma_{in}$  and of dimension  $12.5 \cdot 10^{-3} \times 9 \cdot 10^{-3}$  km<sup>2</sup> as explained in Figure 1. The simulation is carried out between 8 a.m. to 9 a.m., i.e.,  $t \in (0, 1)$  with  $\Delta t = 0.001$  h,  $\rho^0 = 0$ ,  $\|\mathbf{v}(\rho^0)\| = 0$ ,  $v_{max} = 70$  km/h,  $c = 40$  km/h,  $\rho_{max} = 800$  veh/km<sup>2</sup> and  $k = 1$  km<sup>2</sup>/h. The direction of road traffic is fixed in  $\Gamma_{in}$  per  $\mathbf{d}_0 = (1, 0)$  (for  $\theta = 0$ ). The vehicle flow rate

function  $f_{in}$  is computed by  $f_{in}(x, y, t) = f_{max} \times f(t)$ , where  $f_{max} = 9408$  veh/km/h is the maximum flow rate and  $f(t)$  is a positive continuous function defined by:

$$f(t) = \begin{cases} 5t & \text{if } t \in (0 \text{ h}, 0.2 \text{ h}) \\ 1 & \text{if } t \in (0.2 \text{ h}, 0.4 \text{ h}) \\ -3(t - 0.6) + 0.4 & \text{if } t \in (0.4 \text{ h}, 0.6 \text{ h}) \\ 0.4 & \text{if } t \in (0.6 \text{ h}, 1 \text{ h}). \end{cases} \quad (7)$$

In this paper, we are interested in carbon monoxide (CO) generated by road traffic. The characteristic width  $W$  of  $\Omega_p$  is equal to 0.5 km. The chosen wind direction is  $-\pi/4$  (see Figure 2). The physical parameters used are  $\phi^0(x, y) = 0$  kg/km<sup>2</sup>,  $\sigma = 0.6 \cdot 10^{-2}$  h<sup>-1</sup>,  $\mu = 3.5 \cdot 10^{-8}$  km<sup>2</sup>/h,  $\eta = 3.16 \cdot 10^{-5}$  kg/veh/h and  $\nu = 10^{-6}$  kg/veh/km [18].

In the following, we will study the effect of wind on the pollutant transport.

#### 4.1 Stationary wind : $\|\mathbf{u}(x, y, t)\| = 2$ km/h

The peak of the CO concentration, generated before the obstacle, is observed at  $t = 0.4$  h. This is due to a high density of vehicle produced at this time. This density is controlled by the function  $f$  defined in equation (7). Density and concentration decrease over time.

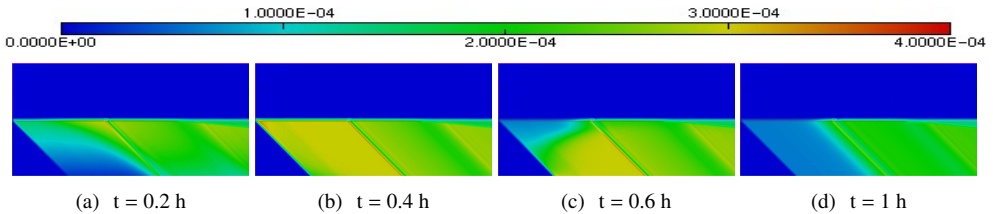


**Figure 3.** Concentration distribution at different times  $t$ .

#### 4.2 Gaussian Model wind: $\|\mathbf{u}(x, y, t)\| = 2 \cdot \exp(-x^2 - y^2)$ km/h

This system is usually located between two rows of buildings. The temporal evolution of the concentration distribution for this system is presented in Figure 4. A significant accumulation

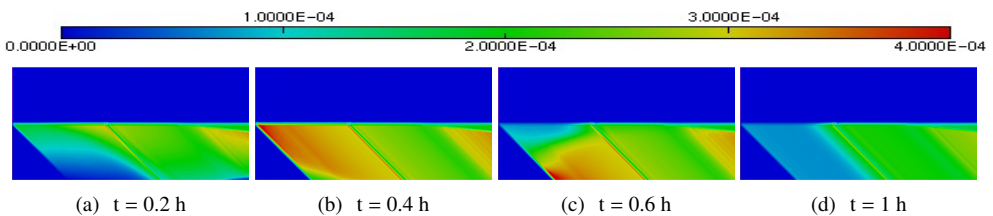


**Figure 4.** Concentration distribution at different times  $t$ .

of pollutants, before the obstacle, compared to Figure 3 is observed at  $t = 0.4$  h and  $t = 0.6$  h. The behavior of the CO concentration is the same after one hour. This shows the effect of the Gaussian model on the evolution of pollutants. The importance of wind shear properties in the development of pollution patterns is highlighted by this study.

### 4.3 Temporal dependence wind velocity

For this study, we choose a sudden change in the magnitude of the wind velocity, the mathematical formulation of which is:

$$g(t) = \begin{cases} 1 & \text{if } t \in (0 \text{ h}, 0.4 \text{ h}) \\ 4 & \text{if } t \in (0.4 \text{ h}, 0.6 \text{ h}) \\ 1 & \text{if } t \in (0.6 \text{ h}, 1 \text{ h}). \end{cases} \quad (8)$$

Figure 5 shows the evolution of the concentration distribution for wind coming from the  $-\pi/4$  direction over a short period  $T = 1$  h. Despite a low density of road traffic at  $t = 0.4$  h and

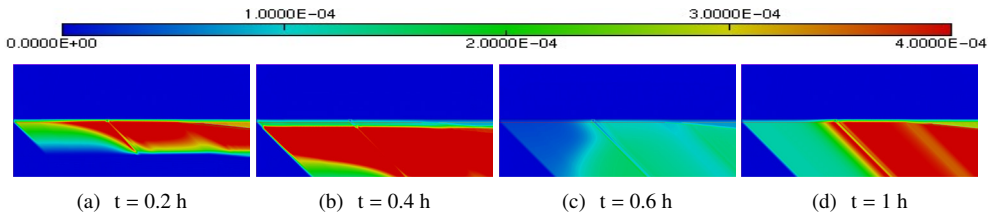


**Figure 5.** Concentration distribution for  $\|\mathbf{u}(x, y, t)\| = g(t)$  at different times  $t$ .

$t = 1$  h, a high concentration of CO is observed before the obstacle and which spreads after. This is due to a low wind speed as indicated by the function  $g(t)$ . The concentration becomes greater at  $t = 0.4$  h, in particular in the southern part of the road, due to a greater density. We can note that wind shear generally has a substantial impact on the horizontal transport of pollutants by extending and tilting polluted plumes. This can change how contaminants are carried from their source, as well as how far they go. Under unstable atmospheric conditions, wind shear can cause eddies to form. That can lead to uneven mixing patterns and possibly higher levels of pollutants in certain areas.

### 4.4 Pollutant concentration over time

In this section, we focus on the study of the temporal evolution of CO concentration at several locations in the domain  $\Omega_p$ . The positions of these locations are denoted by  $A_i, B_i, C_i,$  and  $D_i$  for  $i = 1, 2, 3, 4$ , as shown in Figure 6. Figure 7 shows the evolution concentration over

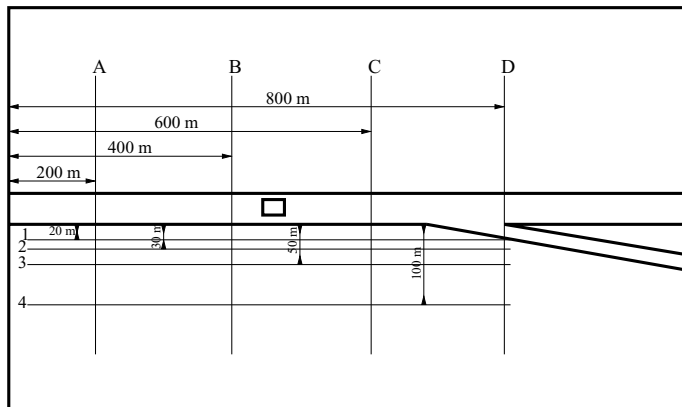


**Figure 6.** Position of  $A_i, B_i, C_i$  and  $D_i$  for  $i = 1, 2, 3, 4$ .

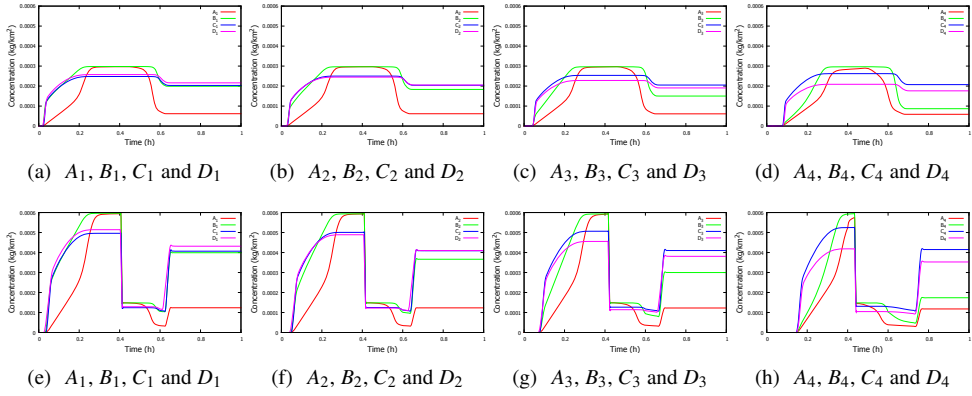


**Figure 7.** Evolution of concentration with  $\|\mathbf{u}(x, y, t)\| = 2$  (a, b, c, d) and  $\|\mathbf{u}(x, y, t)\| = g(t)$  (e, f, g, h).

time for two wind models : stationary, i.e.,  $\|\mathbf{u}(x, y, t)\| = 2$  (a, b, c, d) and sudden change, i.e.,  $\|\mathbf{u}(x, y, t)\| = g(t)$  (e, f, g, h).

To properly analyze the curves, we have divided each one and for each model, into three different regions. For the stationary wind graphics (a, b, c, d), the regions are classified as:

- for  $t \in (0 \text{ h}, 0.2 \text{ h})$  nonlinear growth: A nonlinear evolution is observed for each curve whose shape depends on the position of the chosen points. It is regular thanks to a stationary wind direction and speed.
- for  $t \in (0.2 \text{ h}, 0.6 \text{ h})$  saturation: A stationary concentration is observed due to a significant density in the selected locations.
- for  $t \in (0.6 \text{ h}, 1 \text{ h})$  decrease: The pollutant leaves the area with a characteristic time that is highly dependent on the distance from the obstacle, especially downstream of the congestion, as shown in the graph's last section.

For the abrupt wind change graphics (e, f, g, h), the regions are classified as:

- for  $t \in (0 \text{ h}, 0.2 \text{ h})$  nonlinear growth: The evolution is similar to the first model but with peaks of higher concentration. This is due to a significantly lower wind speed.
- for  $t \in (0.2 \text{ h}, 0.6 \text{ h})$  rapid decrease: We observe a significant and instantaneous decrease in the concentration of pollutants. This is explained by the fact that the wind speed multiplies by 4 during this period. This speed quickly diffuses the pollutants from the selected areas. The evolution is non-linear.
- for  $t \in (0.6 \text{ h}, 1 \text{ h})$  increase: The wind returns to its previous laminar state during this time. The pollutant concentration rise to a particular point.

## 5 Conclusion

In this paper, we have developed a new model of traffic-related air pollution whose pollution source is generated by density of vehicles where the wind velocity magnitude is an input that can vary. The coupled equations are computed via an algorithm combining the characteristics method with the Lagrange-Galerkin method. With this model, we can take account the meteorological conditions. Here, we are specifically interested in studying the problem of horizontal wind shear and the temporal and spatial dependence of wind velocity magnitude. Starting with a laminar, stationary, unidirectional wind, we have easily compared two scenarios of wind magnitudes : Gaussian and sudden shifts over time. The pollutant concentration distribution show that the wind shear significantly affects the horizontal transport of

pollutants. The study of the time evolution of pollutant concentration confirms the nonlinear features behind pollutant diffusion. This work is a first step and could be a reference before adding real wind dynamics by using meteorological databases.

## References

- [1] T. Feng, Y. Sun, Y. Shi, J. Ma, C. Feng, Z. Chen, Air pollution control policies and impacts: A review. *Renew. Sustain. Energy Rev.* **191**, 114071 (2024).
- [2] D.J. Sun, S. Wu, S. Shen, T. Xu, Simulation and assessment of traffic pollutant dispersion at an urban signalized intersection using multiple platforms. *Atmos. Pollut. Res.* **12**, 101087 (2021).
- [3] H. Yang, C. Lu, Y. Hu, P.W. Chan, L. Li, L. Zhang, Effects of horizontal transport and vertical mixing on nocturnal ozone pollution in the Pearl River Delta. *Atmosphere*, **13**, 1318 (2022).
- [4] A.E. Etuman, I. Coll, Integrated air quality modeling for urban policy: A novel approach with olympus-chimere. *Atmos. Environ.* **315**, 120–134 (2023).
- [5] G. Cervone, J. Dallmeyer, A.D. Lattner, P. Franzese, N. Waters, Coupling Traffic and Gas Dispersion Simulation for Atmospheric Pollution Estimation. *CyberGIS for Geospatial Discovery and Innovation*, 13–31 (2019).
- [6] M. Fallahshorshani, M. André, C. Bonhomme, C. Seigneur, Coupling Traffic, Pollutant Emission, Air and Water Quality Models: Technical Review and Perspectives. *Procedia Soc. Behav. Sci.* **48** 1794–1804 (2012).
- [7] F. Della Rossa, C. D'Angelo, A. Quarteroni, A distributed model of traffic flows on extended regions. *Netw. Heterog. Media.* **5**, 525–544 (2010).
- [8] L.M. Romero, F.G. Benitez, Traffic flow continuum modeling by hypersingular boundary integral equations. *Int. J. Numer. Methods Eng.* **82**, 47–63 (2010).
- [9] G.F. Newell, A Theory of Platoon Formation in Tunnel Traffic. *Oper. Res.* **7**, 589–598 (1959).
- [10] R.E. Franklin, The structure of a traffic shock wave. *Civ. Eng. Public Work. Rev.* **56**, 1186–1188 (1961).
- [11] S. Mollier, M.L. Delle Monache, C.C. de Wit, Two-dimensional macroscopic model for large scale traffic networks. *Transp. Res. B Methodol.* **122**, 309–326 (2019).
- [12] H. Bourlès, *Fundamentals of Advanced Mathematics 2: Field Extensions, Topology and Topological Vector Spaces, Functional Spaces, and Sheaves*, (ISTE Press—Elsevier, Amsterdam, 2018).
- [13] Y.N. Skiba, V. Davydova-Belitskaya, On the estimation of impact of vehicular emissions. *Ecol. Model.* **166**, 169–184 (2003).
- [14] E.A. Zakarin, B.M. Mirkarimova, GIS-based mathematical modeling of urban air pollution. *Izv. Atmos. Ocean. Phys.* **36**, 334–342 (2000).
- [15] J. Douglas, T.F. Russel, Numerical Methods for Convection-Dominated Diffusion Problems Based on Combining the Method of Characteristics with Finite Element or Finite Difference Procedures. *SIAM J. Numer. Anal.* **19**, 871–885 (1982).
- [16] H. Borouchaki, P.L. George, *Delauney Triangulation and Meshing: Application to Finite Elements*, (Hermes, Paris, 1998).
- [17] F. Hecht, New development in FreeFem++. *J. Numer. Math.* **20**, 251–265 (2012).
- [18] B. Sportisse, *Fundamentals in Air Pollution: From Processes to Modelling*, (Springer, New York, 2010).